THE EFFECT OF AN EXTERNAL MAGNETIC FIELD ON THE ENTROPY GENERATION IN THREE-DIMENSIONAL NATURAL CONVECTION

by

Lioua KOLSI [*]***, Awatef ABIDI, Mohamed Naceur BORJINI, and Habib BEN AÏSSIA***

Ecole Nationale d'Ingénieur de Monastir, Monastir, Tunisia

Original scientific paper
UDC: 536.25:537.632/.636:519.876.2
DOI: 10.2298/TSCI1002341K

A 3-D original numerical study of entropy generation in the case of liquid metal laminar natural convection in a differentially heated cubic cavity and in the presence of an external magnetic field orthogonal to the isothermal walls is carried out. The effect of this field on the various types of irreversibilities is analyzed. It was observed that in the presence of a magnetic field the generated entropy is distributed on the entire cavity and that the magnetic field limits the 3-D character of the distribution of the generated entropy.

Key words: entropy generation, magnetic field, natural convection

Introduction

Many thermodynamic systems like the heat exchangers, turboshaft engines, electrothermics, and porous media are the subject of the irreversibility phenomena due to heat gradients, friction effects, diffusion, and Joule effect *etc*… The analysis of the second law of thermodynamic has recently gained an important attention in order to minimize these irreversibilties. However, there are few works concerning entropy generation in confined natural convection situations.

Magherbi *et al*. [1] studied numerically the entropy generation for the non-stationary natural convection in square cavity. The results prove that the total generation of entropy reaches a maximum value at the beginning, which increases with the Rayleigh number and the ratio of irreversibility distribution. They noted that the generation of entropy tends asymptotically towards a constant value for low Rayleigh numbers; while an oscillation of the entropy generation was observed for higher Rayleigh numbers, before reaching the balance state. The results evince that by increasing the Rayleigh number, the effect of the viscous irreversibility starts to dominate the irreversibility due to the thermal transfer. In the stationary state, the generation of entropy is distributed on the whole field for small Rayleigh numbers, but it is confined in the vicinity of the active walls for high Rayleigh numbers.

* Corresponding author; e-mail: lioua_enim@yahoo.fr

Erbay *et al.* [2] studied the same problem for partially or completely heated cavity. In the case of the completely heated walls, the active zones of the generated entropy due to the thermal transfer are in the low corner of the hot wall and the top corner of the cold wall. For the selective heating, the active zones are localized in the higher part of the heated section.

Various geometric and thermal boundary configurations are considered in literature. Especially the effect of inclination is considered by Baytas [3] and Magherbi *et al*. [4]. Indeed, the aim of Baytas [3] research is to study the entropy generation in a tilted 2-D saturated porous cavity during the thermal transfer of laminar natural convection. These results prove that when the Rayleigh number falls, the thermal transfer irreversibility starts to dominate the friction one. The number of Bejan is quickly changed for inclination between the angles 150° and 270°.

Magherbi *et al*. [4] carried out a numerical study relating to the generation of entropy due to the thermal transfer, the mass transfer, and the friction. This study is done in the case of the doubles diffusive laminar convection, in an inclined cavity with diffusive walls of heat and mass transfer. The influences of inclination, the number of Grashof, and the ratio of buoyancy on the total generation of entropy were studied. The localization of irreversibilities due to the thermal transfer, the mass transfer, and the friction of the fluid is discussed for three angles of inclination for a fixed Grashof number. The results prove that for moderate Lewis numbers, the total generation of entropy rises when increasing the Grashof number or the buoyancy ratio. Locally, the irreversibility due to heat and mass transfer are almost identical and are localized at the bottom and the top of the heated and cooled walls, respectively.

The impact of the aspect ratio is also considered. Recently, Ilis *et al*. [5] demonstrate that for high Rayleigh number, the total entropy generation raises with increasing aspect ratio, reach a maximum and then decreases. The authors present in addition a complete bibliography on this subject.

It figures also the works of Varol *et al*. [6] concerning a triangular enclosure and Dagtekin *et al*. [7] for Γ-shaped enclosure. The first cited work showed that the sloping wall angle can be used as a parameter to control entropy generation. In fact, the entropy production rises with increasing the sloping wall inclination angle of the triangular enclosure. The second cited work concluded that the height of step is more effective than top face of the heated step in entropy generation. Also the effect of the aspect ratio is not significant for weak Rayleigh numbers.

To end with special configurations it is important to mention the recent study of Famouri *et al*. [8] concerning the effect of vertical position of heated obstacle placed in square enclosure on the local and average entropy generation.

Among a small number of works relating to entropy generation in the case of magnetohydrodynamic natural convection in confined enclosure, it figures the study effectuated by Mahmud and Fraser [9] in the case of saturated porous cavity. The magnetic force is assumed along the direction of the force of gravity. The effect of Rayleigh and Hartmann numbers on the average Nusselt number, the entropy generation number, and Bejan number is examined. The increase in the Hartmann number tends to delay the movement of the fluid inside the cavity. The Nusselt number falls with the increase of Hartmann number. In the absence of the magnetic force, the rate of entropy generation is relatively higher close to the two vertical walls while this rate falls according to Hartmann number.

Entropy generation in magnetohydrodynamic problems is more developed for flow in channels. Ibáñez *et al*. [10] applied the method of minimization of entropy generation to optimize a magnetohydrodynamic flow between two infinite parallel walls having a finished electric conductivity. The authors showed that the generation of entropy reaches a minimum when the walls are cooled in an asymmetrical way. Also Mahmud *et al*. [11], Tasnim *et al*. [12], and Aiboud-Saouli [13] carried out an analysis to study the first and the second laws of thermodynamics of a flow of mixed laminar convection inside a vertical channel under the action of a transverse magnetic field.

Several studies [14-22] were undertaken on the effect of external magnetic field on the natural convection, these studies showed that this field reduces thermal transfer and organizes the flow. These effects are very required in several engineering applications like foundry, solidification and especially in the processes of crystalline growths. However there are few works concerning entropy generation in presence of magnetic field.

Within this framework we study the effect of a magnetic field on these losses of energy in the case of the 3-D natural convection by highlighting the effect of Hartmann number and the irreversibility coefficient. The Prandtl number is fixed at 0.026 and two Rayleigh number are used (Ra = 10^4 and Ra = 10^5). A foremost attention is given to the 3-D character of irreversibilities.

Mathematical formulation and numerical model

Figure 1 schematizes the configuration considered: the left and right walls are differentially heated, the other walls are considered adiabatic, and a homogeneous magnetic field expressed by $B_0\vec{e}_B$ is imposed perpendicular to the heated walls. All the walls of the cavity are considered insulating electrically. Under the effect of this field, electrical currents will be induced in the melt and the flow becomes controlled by, in addition to Rayleigh and Prandtl numbers, two new dimensionless parameters, which are the magnetic Reynolds number:

$$\mathrm{R_m} = \mu\sigma v_0 l$$

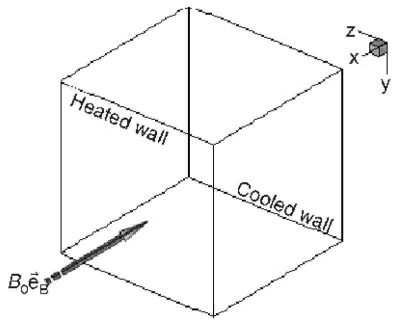

Figure 1. Description of the cavity

and the Hartman number:

$$\mathrm{Ha} \quad \sqrt{\frac{B_0^2 l^2 \sigma}{\rho\nu}}$$

The magnetic Reynolds number represents the ratio between the magnetic field induced by the movement of the fluid and the applied magnetic field. The Hartmann number represents the ratio between Lorentz forces produced by the interaction of the current density $\vec{J}$ with the applied magnetic field $\vec{B}$, and the viscosity forces.

In fact the movement of the fluid is induced by the variations of the density caused by the gradients of temperature. The presence of the magnetic field will cause in its turn a Lorentz force, given by: [22]

$$\vec{F} = \rho_e\vec{E} \quad \vec{J} \quad \vec{B} \tag{1}$$

with $\vec{E} \qquad \vec{\ } \Phi$

In addition, for a moving medium, the density of electrical current is governed by the Ohm law which is written [22]:

$$\vec{J} = \rho_e \vec{V} + \sigma_e(-\vec{\nabla}\Phi + \vec{V} \times \vec{B}) \tag{2}$$

In the case of a molten metal ρ_e is usually very small compare to σ_e, the terms $\rho_e \vec{E}$ and $\rho_e \vec{V}$ in the eqs. (1) and (2) are negligible, $\vec{B}$ is composed by the applied magnetic field $B_0 \vec{e}_B$ and the induced magnetic field produced by the electrical currents. For molten metal $R_m < 10^{-3}$ [23] and we can neglect the induced field so the Hartmann number becomes the only additional parameter related to the external applied magnetic field. In addition to Ohm's law, the density of electrical current $\vec{J}$ is governed by the conservation law:

$$\vec{\nabla} \cdot \vec{J} = 0 \tag{3}$$

Thus by adding the relations relating to the presence of the external magnetic field to those of an ordinary hydrodynamic laminar flow, the equations describing the problem of magnetohydrodynamic natural convection arise in the following way:

$$\vec{\nabla} \cdot \vec{V} = 0 \tag{4}$$

$$\frac{\partial \vec{V}}{\partial t} + (\vec{V} \cdot \vec{\nabla})\vec{V} = -\frac{1}{\rho}\vec{\nabla} P + \frac{1}{\rho}(\vec{J} \times \vec{B}) + \nu \Delta \vec{V} + \beta(T - T_0)\vec{g} \tag{5}$$

$$\frac{\partial T}{\partial t} + \vec{V} \cdot \vec{\nabla} T = \alpha \vec{\nabla}^2 T \tag{6}$$

$$\vec{J} = \sigma_e(-\vec{\nabla}\Phi + \vec{V} \times \vec{B}) \tag{7}$$

$$\vec{\nabla} \cdot \vec{J} = 0 \tag{8}$$

As numerical method we had recourse to the vorticity-vector potential formalism $(\vec{\psi} - \vec{\omega})$ which allows, in a 3-D configuration, the elimination of the pressure, which is a delicate term to treat. To eliminate this term one applies the rotational to the equation of momentum. The vector potential and the vorticity are, respectively, defined by the two following relations:

$$\vec{\omega} = \vec{\nabla} \times \vec{V} \quad \text{and} \quad \vec{V} = \vec{\nabla} \times \vec{\psi}$$

The setting in equation is described with more details in the article of Kolsi *et al.* [14].

After non-dimensionalization of t', $\vec{V}$, $\vec{\psi}$, $\vec{\omega}$, $\vec{J}$, $\vec{B}$, Φ' by l^2/α, α/l, α, l^2/α, $\sigma v_0 B_0$, B_0, $\lambda v_0 B_0$, respectively, the system of equations controlling the phenomenon becomes:

$$-\vec{\omega} = \vec{\nabla}^2 \vec{\psi} \tag{9}$$

$$\frac{\partial \vec{\omega}}{\partial t} + (\vec{V} \cdot \vec{\nabla})\vec{\omega} - (\vec{\omega} \cdot \vec{\nabla})\vec{V} = \Pr \vec{\nabla}^2 \vec{\omega} + \mathrm{Ra}\Pr\left[\frac{\partial T}{\partial z}; 0; -\frac{\partial T}{\partial x}\right] + \mathrm{Ra}\Pr\mathrm{Ha}^2[\vec{\nabla} \times (\vec{J} \times \vec{e}_B)] \tag{10}$$

$$\frac{\partial T}{\partial t} + \vec{V} \cdot \vec{\nabla} T = \vec{\nabla}^2 T \tag{11}$$

$$\vec{J} = -\vec{\nabla}\Phi + \vec{V} \times \vec{e}_B \tag{12}$$

$$\vec{\nabla}^2 \Phi = \vec{\nabla} \cdot (\vec{V} \times \vec{B}) = \vec{e}_B \cdot \vec{\omega} \tag{13}$$

with $\Pr = \nu/\alpha$ and $\mathrm{Ra} = (g\beta\Delta T l^3)/\nu\alpha$; $\Delta T = T'_h - T'_c$.

The boundary conditions are given as:

– temperature

$$T = 1 \text{ at } x = 1, \ T = 0 \text{ at } x = 0$$

$$\frac{\partial T}{\partial n} \quad 0 \text{ on other walls}$$

– vorticity

$$\omega_{x} 0, \quad \omega_{y} \quad \frac{\partial V_{z}}{\partial x}, \quad \omega_{z} \quad \frac{\partial V_{y}}{\partial x} \quad \text{at} \quad x \quad 0 \text{ and } 1$$

$$\omega_{x} \quad \frac{\partial V_{z}}{\partial y}, \quad \omega_{y} \quad 0, \quad \omega_{z} \quad \frac{\partial V_{x}}{\partial y} \quad \text{at} \quad y \quad 0 \text{ and } 1$$

$$\omega_{x} \quad \frac{\partial V_{z}}{\partial y}, \quad \omega_{y} \quad \frac{\partial V_{x}}{\partial z}, \quad \omega_{z} \quad 0 \quad \text{at} \quad z \quad 0 \text{ and } 1$$

– vector potential

$$\frac{\partial \psi_{x}}{\partial x} \quad \psi_{y} \quad \psi_{z} \quad 0 \quad \text{at} \quad x \quad 0 \text{ and } 1$$

$$\psi_{x} \quad \frac{\partial \psi_{y}}{\partial y} \quad \psi_{z} \quad 0 \quad \text{at} \quad y \quad 0 \text{ and } 1$$

$$\psi_{x} \quad \psi_{y} \quad \frac{\partial \psi_{z}}{\partial z} \quad 0 \quad \text{at} \quad z \quad 0 \text{ and } 1$$

– velocity

$$V_{x} = V_{y} = V_{z} = 0 \text{ on all walls}$$

– electric potential

$$\Phi / \ n = 0 \text{ on all walls}$$

– current density

$$\vec{J}\vec{n} \quad 0 \text{ on all walls}$$

where $\vec{n}$ is the unit vector normal to the wall.

In the presence of a magnetic field the generated entropy is written in the following form [11]:

$$S_{gen} \quad \frac{1}{T^{2}} \vec{q} \ \vec{\ } T \quad \frac{\mu}{T} \phi \quad \frac{1}{T} (\vec{J} \quad \rho_{e} \vec{V})(\vec{E} \quad \vec{V} \quad \vec{B}) \tag{14}$$

where $\rho_{e}\vec{V}$ is negligible and $\vec{q} \quad k \ T$. The first term represents the generated entropy due to temperature gradient, the second that due to the friction effects, and the last that due to the presence of the magnetic field.

The dissipation function in incompressible flow is written as:

$$\phi \quad 2 \quad \frac{\partial V_{x}}{\partial x}^{2} \quad \frac{\partial V_{y}}{\partial y}^{2} \quad \frac{\partial V_{z}}{\partial z}^{2}$$

$$\frac{\partial V_{y}}{\partial x} \quad \frac{\partial V_{x}}{\partial y}^{2} \quad \frac{\partial V_{z}}{\partial y} \quad \frac{\partial V_{y}}{\partial z}^{2} \quad \frac{\partial V_{x}}{\partial z} \quad \frac{\partial V_{z}}{\partial x}^{2} \tag{15}$$

from where the generated entropy is written:

$$S_{\mathrm{gen}} = \frac{k}{T^2}\left[\left(\frac{\partial T}{\partial x}\right)^2 + \left(\frac{\partial T}{\partial y}\right)^2 + \left(\frac{\partial T}{\partial z}\right)^2\right] + \frac{2\mu}{T}\left[\left(\frac{\partial V_{\mathrm{x}}}{\partial x}\right)^2 + \left(\frac{\partial V_{\mathrm{y}}}{\partial y}\right)^2 + \left(\frac{\partial V_{\mathrm{z}}}{\partial z}\right)^2\right] +$$
$$+ \frac{\mu}{T}\left[\left(\frac{\partial V_{\mathrm{y}}}{\partial x} + \frac{\partial V_{\mathrm{x}}}{\partial y}\right)^2 + \left(\frac{\partial V_{\mathrm{z}}}{\partial y} + \frac{\partial V_{\mathrm{y}}}{\partial z}\right)^2 + \left(\frac{\partial V_{\mathrm{x}}}{\partial z} + \frac{\partial V_{\mathrm{z}}}{\partial x}\right)^2\right] + \frac{1}{T}\frac{1}{\sigma_{\mathrm{e}}}(J_{\mathrm{x}}^2 + J_{\mathrm{y}}^2 + J_{\mathrm{z}}^2) \tag{16}$$

After a dimensionalisation one obtains generated entropy number (dimensionless local generated entropy) which is written in the following way:

$$N_{\mathrm{S}} = S_{\mathrm{gen}}\frac{1}{k}\left(\frac{lT_{\mathrm{m}}}{\Delta T}\right)^2 \tag{17}$$

from where:

$$N_S = \left[\left(\frac{\partial T}{\partial x}\right)^2 + \left(\frac{\partial T}{\partial y}\right)^2 + \left(\frac{\partial T}{\partial z}\right)^2\right] + \varphi\left\{2\left[\left(\frac{\partial V_{\mathrm{x}}}{\partial x}\right)^2 + \left(\frac{\partial V_{\mathrm{y}}}{\partial y}\right)^2 + \left(\frac{\partial V_{\mathrm{z}}}{\partial z}\right)^2\right] +\right.$$
$$\left. + \left[\left(\frac{\partial V_{\mathrm{y}}}{\partial x} + \frac{\partial V_{\mathrm{x}}}{\partial y}\right)^2 + \left(\frac{\partial V_{\mathrm{z}}}{\partial y} + \frac{\partial V_{\mathrm{y}}}{\partial z}\right)^2 + \left(\frac{\partial V_{\mathrm{x}}}{\partial z} + \frac{\partial V_{\mathrm{z}}}{\partial x}\right)^2\right]\right\} + \varphi\mathrm{Ha}^2(J_{\mathrm{x}}^2 + J_{\mathrm{y}}^2 + J_{\mathrm{z}}^2) \tag{18}$$

With φ is the irreversibility coefficient:

$$\varphi = \frac{\mu\alpha^2 T_{\mathrm{m}}}{l^2 k\Delta T^2} \tag{19}$$

The first term of N_{S} represents the local irreversibility due to the temperatures gradients (it is noted $N_{\mathrm{S\text{-}th}}$). The second term represents the contribution of the viscous effects in the irreversibility (it is noted $N_{\mathrm{S\text{-}fr}}$), and the third term represents the generated local entropy due to the Joule effect (it is noted $N_{\mathrm{S\text{-}J}}$). N_{S} give a good idea on the profile and the distribution of the generated local dimensionless entropy. The total dimensionless generated entropy is written:

$$S_{\mathrm{tot}} = \int_V N_{\mathrm{S}}\mathrm{d}v = \int_V (N_{\mathrm{S\text{-}th}} + N_{\mathrm{S\text{-}fr}} + N_{\mathrm{S\text{-}J}})\mathrm{d}v = S_{\mathrm{th}} + S_{\mathrm{fr}} + S_{\mathrm{J}} \tag{20}$$

Equations governing the problem are discretized using the finite volume method with a central difference scheme. The order of resolution of the equations is successively equation of continuity, energy, momentum, Ohm's law, and conservation of electric charge. More information on the numerical method is in the work of Borjini *et al.* [15].

Results and discussion

In this study, the Prandtl number is fixed at Pr = 0.026 relating to mercury, two Rayleigh number are used – Ra =10^4 and Ra = 10^5, and the Hartmann number lies between 0 and 150. The irreversibility coefficient lies between 10^{-4} and 10^{-1}. A particular interest is given to the study of the 3-D distribution of the generated entropy and to the effect of the magnetic field on different types of the irreversibilities. A uniform spatial grid of 51^3 nodes and a dimensionless time step equal to 10^{-4} are used. The solution is considered acceptable when the following convergence criterion is satisfied for each step of time and for each dependent variable:

$$\frac{\max\left|\Delta^{m} \quad \Delta^{m \ 1}\right|}{\max\left|\Delta^{m}\right|} \quad 10^{\ 5} \tag{21}$$

where the superscript m designates the iteration number.

Flow structure

Figure 2 presents the flow structure for various Hartmann numbers (on half of the cavity), one notices for Ha = 0, a one vortex flow structure and a spiraling transversal disordered flow. By increasing Ha, the transversal flow becomes more and more ordered, such is the case for Ha = 50. For Ha = 60, the flow structure presents two vortices, a more detailed description is reported in [14].

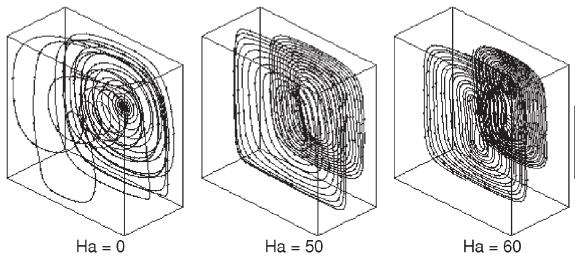

Figure 2. Some particle tracks for Ra = 10^4 and different Hartmann numbers

Various types of irreversibilities

Figure 3 represents the variation of the total generated entropy as function of Hartmann number for different irreversibility coefficient. It is noticed that for $\varphi = 10^{-1}$, $\varphi = 10^{-2}$, and $\varphi = 10^{-3}$, the generated entropy increase then decrease by increasing Ha. For $\varphi = 10^{-4}$ the growing zone does not exist any more. This attenuation is explained by the magnetic damping of the flow. It is also noticed that the maximum of S_{tot} occurs for 15 < Ha < 20 for all considered values of φ.

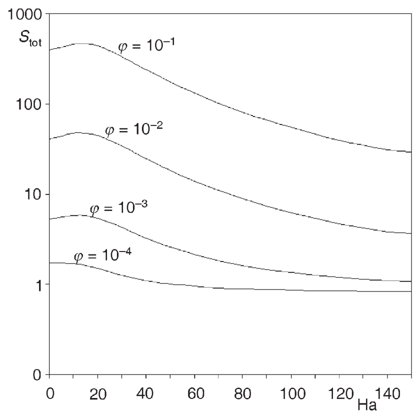

Figure 3. Variation of the total generated entropy as function of Ha; Ra = 10^4

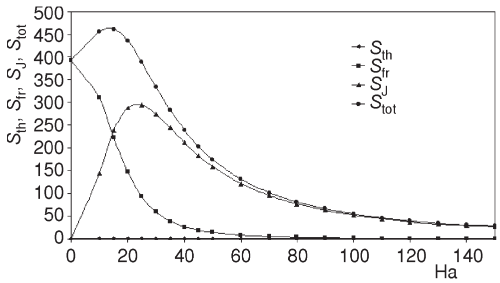

Figure 4. Variation of generated entropy as function of Ha; $\varphi = 10^{-1}$, Ra = 10^4

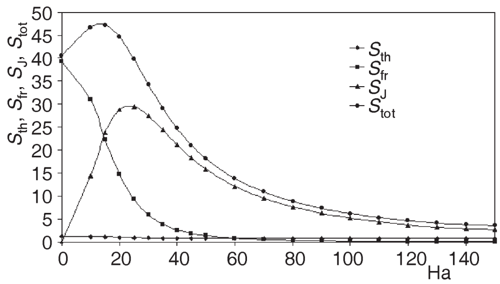

Figure 5. Variation of generated entropy as function of Ha; $\varphi = 10^{-2}$, Ra = 10^4

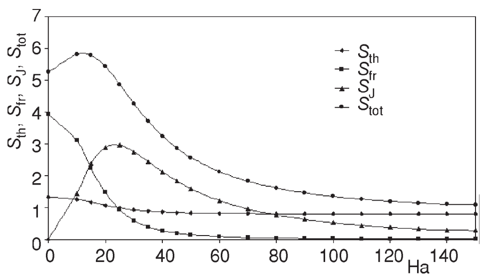

Figure 6. Variation of generated entropy as function of Ha; $\varphi = 10^{-3}$, Ra = 10^4

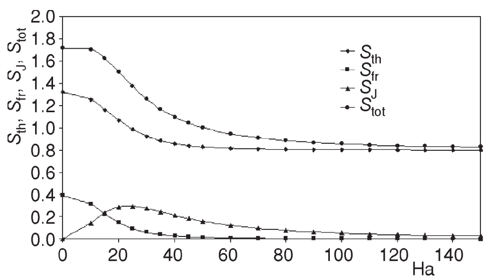

Figure 7. Variation of generated entropy as function of Ha; $\varphi = 10^{-4}$, Ra = 10^4

Figures 4, 5, 6, and 7 present, for various irreversibility coefficients, the variation of S_{th}, S_{fr}, S_J and S_{tot} according to Ha. One notices that S_{th} and S_{fr} decrease according to Ha, but S_J presents a maximum. From where the maximum in the variation of the total generated entropy according to Ha is due to the dissipation by Joule effect. This result is also met in the 2-D channel flow [10].

By analyzing these figures, one notices that for $\varphi = 10^{-1}$ and $\varphi = 10^{-2}$ the generated entropy due to the thermal transfer is negligible compared to that due to the viscous effects and the Joule effect. For $\varphi = 10^{-3}$, one notices that S_{th} becomes of the same order of magnitude as S_{fr} and S_J. For $\varphi = 10^{-4}$ the generated entropy due to the variation in temperature becomes dominant.

Figures 4, 5, 6 and 7 also show that the effect of the magnetic field is more considerable on S_{fr} and S_J that on S_{th} and show that S_J presents a maximum for all the values of φ.

3-D distribution of the irreversibilities

In order to analyze the 3-D aspect of the entropy generation we traced for two values of the total generated entropy for Ha = 0, Ha = 50, and Ha = 100 (fig. 8). The 3-D behavior is more important for Ha = 0 for both $\varphi = 10^{-1}$ and $\varphi = 10^{-4}$. For $\varphi = 10^{-1}$ the generated entropy occurs principally near the active walls for both moderately and highly damped flow. As predicted and for $\varphi = 10^{-4}$ and Ha = 0, the creation of entropy is mainly localized near the bottom of the hot surface and the top of the cold surface.

Figure 9 presents for Ha = 0 and Ha = 50 the distribution of the local total generated entropy in the z = 0.5 (in continued lines) and z = 0.9 (in dashed lines) plans for different values of the irreversibility coefficient. This figure confirms that the magnetic field limits the 3-D character of the distribution of the generated entropy for all value of φ. This 3-D behavior is clear for $\varphi = 10^{-3}$and Ha = 0.

Figures 10 and 11 represent, respectively, for Ha = 0 and Ha = 50 a decomposition of the distribution of total generated entropy for φ= 10^{-1}, in plans z = 0.5 and z = 0.9. For Ha = 0, S_{tot} is broken up into S_{th} and S_{fr}. For Ha = 50, S_{tot} is broken up into S_{th}, S_{fr}, and S_J.

These figures show that for Ra = 10^4 and Ha = 0, the distribution of S_{tot} (fig. 9) is very similar to the iso-entropies due to frictions, fig. 10(a), what indicates the predominance of the irreversibility due to the viscous effects. For Ra =10^5 generated entropies are more concentrated (than Ra = 10^4) near the actives walls, for both Ha = 0 and Ha = 50.

By decreasing (fig. 9) the distribution approaches with the iso-entropies due to temperature gradient what indicates the predominance of the irreversibility due to the thermal transfer.

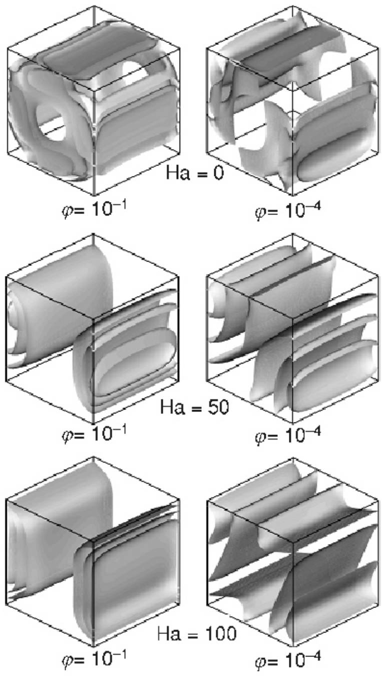

Figure 8. Iso-surfaces of the total generated entropy as function of φ and Ha; Ra = 10^4

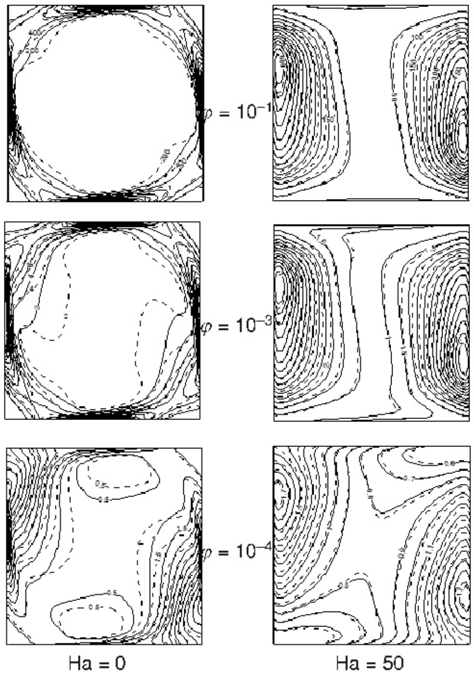

Figure 9. Contours of total generated entropy; in continuous lines z = 0.5 plan; in dashed lines z = 0.9 plan; Ra = 10^4

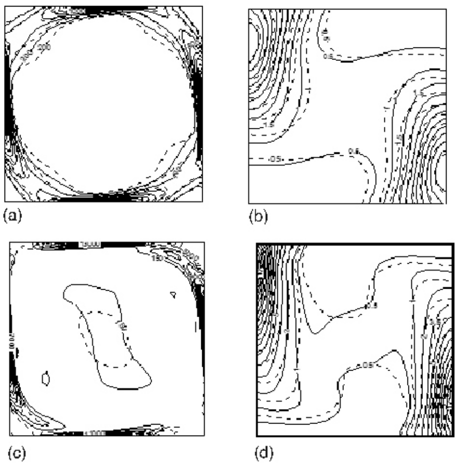

Figure 10. Contours of generated entropy for Ha = 0 and φ = 10^{-1}
(a) due to friction for Ra = 10^4; (b) due to temperature variations for Ra = 10^4; (c) due to friction for Ra = 10^5; (d) due to temperatures variations for Ra = 10^5; in continuous lines z = 0.5 plan; in dashed lines: z = 0.9 plan

The 3-D character exists for both S_{th} and S_{fr}. This is also noticed that for low coefficient of irreversibility the generated entropy covers all the z = 0.5 plan. By increasing the coefficient of irreversibility, the generated entropy concentrates (locates itself) along the walls of the cavity. The important generation of S_{fr} is located near the center of the faces. The generation of S_{th} is near the top corner of the hot wall and the bottom of the cooled wall.

For Ha = 50, in fig. 11, the generated entropy is distributed on all the cavity and non-localised near walls even for $\varphi = 10^{-1}$, which implies that the magnetic field is opposed to the boundary layer phenomenon met for the great Rayleigh numbers. It is also noticed that iso-contours of entropy in the z = 0.5 and z = 0.9 plans are almost coincided except its friction contribution. This can be explained by the bi-dimensionalisation of the flow under the effect of the magnetic field. The 3-D behavior

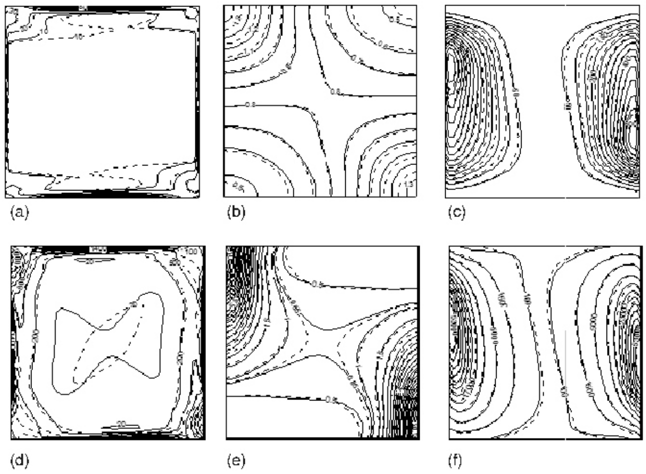

Figure 11. Contours of generated entropy for Ha = 50 and $\varphi = 10^{-1}$ *(a) due to friction for Ra = 10^4; (b) due to temperature variations for Ra = 10^4; (c) due to the Joule effects for Ra = 10^4; (d) due to friction for Ra = 10^5; (e) due to temperature variations for Ra = 10^5; (f) due to the Joule effects for Ra = 10^5; in continuous lines z = 0.5 plan; in broken lines z = 0.9 plan*

of the distribution of the generated entropy is important for only the S_{fr}. The maximum of S_J is located in the region near the center of active walls.

Figures 12 and 13 present, respectively, for Ra = 10^4 and Ra = 10^5 a decomposition of the generated entropy for different value of Ha. These figures show that by increasing Ha, S_{th} becomes distributed on all the cavity specifically in low Rayleigh number, S_{fr} concentrates close to the higher and lower walls, and S_J always is concentrated near the active walls. These phenomena are more marked for Ra = 10^4 than for Ra = 10^5.

Figures 12 and 13 also show that the 3-D character is more pronounced for the entropy generated due to the viscous effects than the other types of irreversibilities.

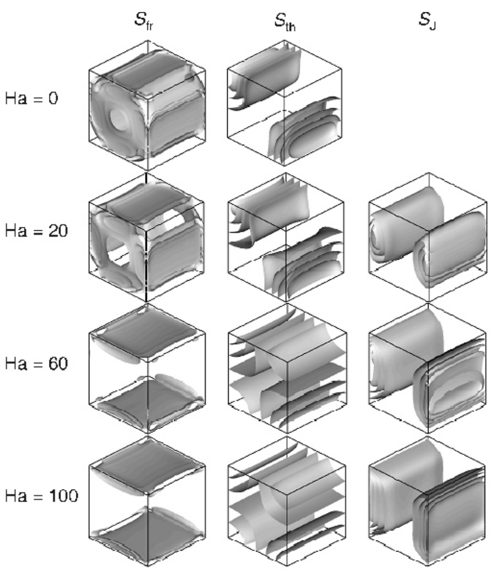

Figure 12. Decomposition of generated entropy for Ra = 10^4 and $\varphi = 10^{-1}$

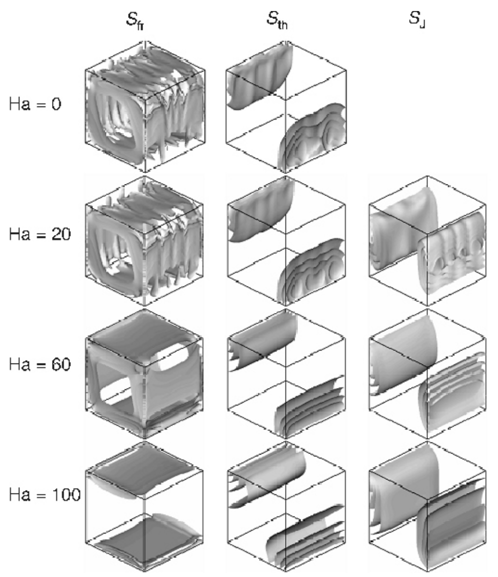

Figure 13. Decomposition of generated entropy for Ra = 10^5 and $\varphi = 10^{-1}$

Conclusions

A study concerning the effect of the presence of a magnetic field on the production of entropy in the case of the natural convection of a low Prandtl liquid metal in a cubic cavity was conducted. This field is applied orthogonally to the isothermal vertical and opposing walls. Some conclusions can be resumed.

In the presence of a magnetic field the generated entropy is distributed on the entire cavity and non-localized in the vicinity of the walls, which implies that the magnetic field is opposed to the boundary layer phenomenon met for the great Rayleigh numbers.

The generated entropy presents a maximum for 10 < Ha < 20 for all considered values of irreversibility coefficient. This range must be avoided when aiming the magnetic damping of the flow.

The magnetic field limits the 3-D character of the distribution of the generated entropy. This character is more pronounced for the entropy generated due to viscous effects.

The entropy generated by friction and Joule effect is more influenced by the magnetic field than that generated by thermal dissipation.

Nomenclature

$\vec{B}$ – dimensionless magnetic field ($= \vec{B}/B_0$)
B_0 – downward component of the magnetic force, [Wbm^{-2}]
$\vec{E}$ – dimensionless electric field
$\vec{e}_B$ – direction of the magnetic field
$\vec{g}$ – acceleration of gravity
Ha – Hartmann number $\{= [(B_0^2 l^2 \sigma)/(\rho\nu)]^{1/2}\}$, [–]
$\vec{J}$ – dimensionless density of electrical current ($= \vec{J}/\sigma v_0 B_0^2$)
k – thermal conductivity, [$\mathrm{Wm}^{-1}\mathrm{K}^{-1}$]
l – enclosure width, [m]
N_s – local generated entropy
$\vec{n}$ – unit vector normal to the wall
P' – pressure, [Pa]
Pr – Prandtl number ($= \nu/\alpha$), [–]
$\vec{q}$ – heat flux vector, [W]
Ra – Rayleigh number ($= g\beta\Delta T l^3/\nu\alpha$), [–]
R_m – magnetic Reynolds number ($= \mu\sigma v_0 l$), [–]
S_{gen} – generated entropy
T – dimensionless temperature [$= (T' - T_c)/(T_k \quad T_c)$]
T_c – cold temperature, [K]
T_h – hot temperature, [K]
t – dimensionless time ($= t'\alpha/l^2$)
$\vec{V}$ – dimensionless velocity vector ($= \vec{V} l/\alpha$)

Greek letters

α – thermal diffusivity, [$\mathrm{m^2s^{-1}}$]
β – expansion coefficient, [$\mathrm{K^{-1}}$]
μ – dynamic viscosity, [Pa·s]
μ_P – magnetic permeability, [$\mathrm{Hm^{-1}}$]
ν – kinematic viscosity, [$\mathrm{m^2s^{-1}}$]
υ_0 – characteristic speed of fluid ($= \alpha/l$)
ρ – density [$\mathrm{kgm^{-3}}$]
ρ_e – density of electric charge, [$\mathrm{Cm^{-3}}$]
σ_e – electric conductivity, [$\Omega^{-1}\mathrm{m}^{-1}$]
φ – irreversibility coefficient
ϕ' – dissipation function
Φ – dimensionless electric potential ($= \Phi'/l\upsilon_0 B_0$)
$\vec{\psi}$ – dimensionless stream function ($= \vec{\psi}'/\alpha$)
$\vec{\omega}$ – dimensionless vorticity ($= \vec{\omega}'\alpha/l^2$)

Subscripts

x, y, z – Cartesian co-ordinates
th – thermal
fr – friction
J – Joule
tot – total

Superscript

′ – dimensional variable

References

[1] Magherbi, M., *et al.*, Second Law Analysis in Convective Heat and Mass Transfer, *Entropy, 8* (2006), 1, pp. 1-17

[2] Erbay, L. B., Altaç, Z., Sülüs, B., An Analysis of the Entropy Generation in a Square Enclosure, *Entropy, 5* (2003), 5, pp. 496-505
[3] Baytas, A. C., Entropy Generation for Natural Convection in an Inclined Porous Cavity, *Int. J. Heat Mass Transfer, 43* (2000), 12, pp. 2089-2099
[4] Magherbi, M., Abbassi, H., Ben Brahim, A., Entropy Generation at the Onset of Natural Convection, *Int. J. Heat Mass Transfer, 46* (2003), 18, pp. 3441-3450
[5] Ilis, G., Mobedi, M., Sunden, B., Effect of Aspect Ratio on Entropy Generation in a Rectangular Cavity with Differentially Heated Vertical Walls, *Int. Comm. Heat and Mass Transfer, 35* (2008), 6, pp. 696-703
[6] Varol, Y., Oztop, H. F., Koca, A., Entropy Production Due to Free Convection in Partially Heated Isosceles Triangular Enclosures, *Applied Thermal Engineering, 28* (2008), 11-12, pp. 1502-1513
[7] Dagtekin, I., Oztop, H. F., Bahloul, A., Entropy Generation for Natural Convection in Γ-Shaped Enclosures, *Int. Comm. Heat and Mass Transfer, 34* (2007), 4, pp. 502-510
[8] Famouri, M., Hooman, K., Entropy Generation for Natural Convection by Heated Partitions in a Cavity, *Int. Comm. Heat and Mass Transfer, 35* (2008), 4, pp. 492-502
[9] Mahmud, S., Fraser, R., Magnetohydrodynamic Free Convection and Entropy Generation in a Square Porous Cavity, *Int. J. Heat Mass Transfer, 47* (2004), 14-16, pp. 3245-3256
[10] Ibáñez, G., Cuevas, S., de Haro, M. L., Optimization of a Magnetohydrodynamic Flow Based on the Entropy Generation Minimization Method, *Int. Comm. Heat and Mass Transfer, 33* (2006), 3, pp. 295-301
[11] Mahmud, S., Tasnim, S. H., Mamun, M. A. H., Thermodynamic Analysis of Mixed Convection in a Channel with Transverse Hydromagnetic Effect, *Int. J. Thermal Science, 42* (2003), 8, pp. 731-740
[12] Tasnim, S. H., Shohel, M., Mamun, M. A. H., Entropy Generation in a Porous Channel with Hydromagnetic Effect, *Exergy, 2* (2002), 4, pp. 300-308
[13] Aïboud-Saouli, S., *et al*., Second-Law Analysis of Laminar Fluid Flow in a Heated Channel with Hydromagnetic and Viscous Dissipation Effects, *Applied Energy, 84* (2007), 3, pp. 279-289
[14] Kolsi, L., *et al*., Effect of an External Magnetic Field on the 3-D Unsteady Natural Convection in a Cubical Enclosure, *Numerical Heat Transfer, Part A, 51* (2007), 10, pp. 1003-1021
[15] Borjini, M. N., *et al*., Hydromagnetic Double-Diffusive Laminar Natural Convection in a Radiatively Participating Fluid, *Numerical Heat Transfer A, 48* (2005), 5, pp. 483-506
[16] Ben Hadid, H., Henry, D., Numerical Study of Convection in the Horizontal Bridgman Configuration under the Action of a Constant Magnetic Field, Part 2, Three Dimensional Flow, *J. Fluid Mech., 333* (1996), 1, pp. 57-83
[17] Mossner, R., Muller, U., A Numerical Investigation of Three-Dimensional Magnetoconvection in Rectangular Cavities, *Int. J. Heat Mass Transfer, 42* (1999), 6, pp. 1111-1121
[18] Di Piazza, I., Ciofalo, M., MHD Free Convection in a Liquid-Metal Filled Cubic Enclosure-I-Differential Heating, *Int. J. Heat Mass Transfer, 45* (2002), 7, pp. 1477-1492
[19] Tagawa, T., Ozoe, H., The Natural Convection of Liquid Metal in a Cubical Enclosure with Various Electro-Conductivities of the Wall under the Magnetic Field, *Int. J. Heat Mass Transfer, 41* (1998), 13, pp. 1917-1928
[20] Kenjereš, S., Hanjalić, K., Numerical Simulation of Magnetic Control of Heat Transfer in Thermal Convection, *Int. J. Heat Fluid Flow, 25* (2004), 3, pp. 559-568
[21] Ozoe, H., Okada, K., Experimental Heat Transfer Rates of Natural Convection of Molten Gallium Suppressed under an External Magnetic Field in either x, y or z Direction, *Int. J. Heat Mass Transfer, 114* (1992), 1, pp. 107-114
[22] Ozoe, H., Okada, K., The Effect of the Direction of the External Magnetic Field on the Three-Dimensional Natural Convection in a Cubical Enclosure, *Int. J. Heat Mass Transfer, 32* (1989), 10, pp. 1939-1954
[23] Saris, I. E., *et al.*, On the Limits of Validity of the Low Magnetic Reynolds Number Approximation in MHD Natural-Convection Heat Transfer, *Numerical Heat Transfer, Part B: Fundamentals, 50* (2006), 2, pp. 157-180

Paper submitted: September 6, 2009
Paper revised: October 27, 2009
Paper accepted: November 25, 2009